The Journal of Animal & Plant Sciences, 26(1): 2016, Page: 233-241
ISSN: 1018-7081

RESPONDING PROTEINS FOR HACAT CELLS AGAINST 2,4-DINITROBENZENE SULFONIC ACID STIMULATIONJA PROTEOMIC STUDY

Ming-Zhong Sun[1], Chunmei Guo[1], Yuling Yin[1], Jintao Lin[1] and Shuqing Liu[2,3,*]

[1] Department of Biotechnology,[2] Department of Biochemistry and Molecular Biology,[3]Provincial Key Laboratory of Cell and Molecular Biology, Dalian Medical University, Dalian,116044, China
[*]Corresponding author's E-mail: lsqsmz@163.com

ABSTRACT

2,4-dinitrobenzene sulfonic acid (DNBS) contributes to the incidences of allergic dermatitis, inflammatory enteritis and colon cancer. In this study, the responding proteins of human keratinocyte HaCaT cells against DNBS stimulation were separated by two-dimensional difference in gel electrophoresis(2DDIGE), quantified by DeCyder software, post-stained by Deep Purple. And the tryptic digested proteins were identified by high performance liquid chromatography combined to nano-electro-spray ionization tandem mass spectrometry (HPLC-nESI-MS/MS) or matrix-assisted laser adsorption ionization (MALDI) MS. Six most up-regulated proteins in HaCaT against DNBS stimulation were chromosome X ORF 26 (Cxorf26), co-chaperone P23 (PTGES3), calmodulin (CALM3), interferon-gamma inducing factor precursor (IL-18), smooth muscle/non-muscle myosin alkali light chain (MYL6)and breakpoint cluster region protein 1 (BANF1). Two most down-regulated proteins were elongin B isoform alpha (TCEB2) and ribosomal protein L23 (RPL23). Their level changes were further validated by Western blotting and qRT-PCR assays. DNBS affects HaCaT proteome. Most of identified protein candidates were reported for the first time to be involved in skin cell damage to chemical stimulation. This work contributes to the understandings of risk assessment and toxicological mechanism of skin diseases caused by chemical carcinogens.

Keywords: DNBS**,** HaCaT**,** DIGE**,** proteomics.

INTRODUCTION

Skin is a target organ for external offenders, such as UV irradiations, ionizing radiations and chemical toxicities (Petrova *et al.*, 2011; Vicentini and Simi, 2008; Yanti and Hwang, 2010). Skin disease has become a major disease seriously threatening public health (Damian *et al*., 2008; Hopper *et al.*, 2009; Housman *et al.*, 2003). The new cases of skin cancers diagnosed each year is equivalent to the incidence of malignancies happen in all other organs combined (Katiyar 2007). The constant increases in life expectancy as well as changes in environmental conditions, dietary habits and lifestyle are contributed to the development of skin diseases (Damian *et al*., 2008; Hensbergen *et al*., 2005; Hopper *et al.*, 2009; Housman *et al*., 2003; Katiyar 2007).

The widespread use and exposure of chemical carcinogens is one of the major causes of skin diseases (Harper 2004; Housman *et al.*, 2003). 2,4-dinitrobenzene sulfonic acid (DNBS), a member of nitrosulfonic acids, is widely used in the industries of faded plating, dye and paint. It can cause allergic dermatitis, inflammatory enteritis, colon cancer and other diseases (Guzzocrea*et al*., 2001; Rijinierse *et al.*, 2006). The incidences of skin cancer, allergic dermatitis and stomach cancer significantly increase for field workers due to long- term exposure to chemical allergens (Guzzocrea *et al*., 2001; Harper 2004). The study on skin cell damage and skin diseases caused by chemical carcinogens at protein level is poorly performed. The molecular mechanisms of skin damages and diseases induced by DNBS stimulation are unknown.

Proteomics has emerged as a promising tool to target differentially expressed proteins, to screen novel targets and create possible therapeutic interventions for human diseases. HaCaT cells are immortalized human keratinocyte cell owing similar differentiation properties with nice proliferation ability and high stability and have been used as the ideal experimental replacements for normal keratinocytes. In current work, two-dimensional difference in gel electrophoresis (2D DIGE) was performed to screen the potential protein targets in HaCaT responding to DNBS stimulation. Deep Purple fluorescent staining was performed for post-electrophoresis gel. Most protein candidates were revealed for the first time to be involved in skin cell damage from chemical carcinogen. This work might provide new insight into the understanding of risk assessment and toxicological mechanism of skin diseases caused by chemical carcinogens.

MATERIALS AND METHODS

Chemicals and instruments: RPMI 1640 and FBS were from Gibco (US). Cy2, Cy3, Cy5, Deep Purple, pH 3-10 NL IPG strip (24cm),1,4-dithiothreitol (DTT),

Acrylamide (Acr), carrier ampholyte, lysine, sodium dodecyl sulfate (SDS), N,N'-methylenebisacrylamide (Bis), 2D-Quant protein assay kit, thiourea and urea were obtained from GE Healthcare (US). Ammonia bicarbonate (ABC), ammonium persulfate (AP), acetronitrile (ACN), 3-[(3-cholamidopropyl)dimethyl-ammonio]-1-propane sulfonate (CHAPS),DNBS, formic acid (FA), iodoacetamide (IAM), and cell lysis solution were from Sigma (US). Modified trypsin was from Promega (Madison, US). All other chemicals were of analytical grade.

Ettan IPG phor II, DeCyder 6.5, Typhoon 9400 scanner and Ettan Spot Picker were from GE (US).C18 column (150 × 0.075mm) was from Dionex (US). LTQ mass spectrometer and TurboSequest Bioworks were from Thermo Finnigan (US). ProOTOF 2000 mass spectrometer was from Perkins Elmer (US).

Cell culture: HaCaT cells were incubated in 90% RPMI1640 supplemented with penicillin/streptomycin, 10% FBS at 37°C with 5% CO_2 for 18 h and then treated with 0.05% DNBS for 2 h. The medium was removed and HaCaT cells were washed 3 times with 20 mM Tris-HCl (pH 7.4). Immediately, the cells were further incubated in fresh 90% RPMI 1640 containing 10% FBS for 6 h. The control HaCaT cells were not treated with 0.05% DNBS.

Protein extraction: Cell pellets were obtained at 3, 000 rpm for 5 min. The cells were then suspended and sonicated in ice-cold lysis buffer (7 Murea, 2 Mthiourea, 4% CHAPS, 30 mM Tris, a cocktail of protease inhibitor mixture). Supernatants were collected by centrifugation at 12,000 rpm for 15 min at 4°C. Proteins were extracted from three batches of cultures. Protein concentrations were determined using 2D Quant protein assay kit. The control and DNBS-treated samples were marked as C1, C2, C3, DNBS1, DNBS2 and DNBS3.

2D DIGE: Samples were labeled using minimal CyDye labeling according to our method (Liu *et al.*, 2008; Sun *et al.*, 2009). Equal amounts of protein extracts from each sample (total of 6) were pooled, and labeled with Cy2 as the internal standard, while Cy3 or Cy5 were used to label experimental or control samples (Table 1). Briefly, protein (50 μg) was labeled with 400 pmol of amine reactive cyanine dye. Labeling reactions were performed on ice in darkness for 30 min before quenched with 10 mM lysine. Unlabeled protein samples 150 μg were mixed with labeled protein (Table 1).The combined samples were then diluted with 2×rehydration buffer (7 M urea, 2 M thiourea, 4% CHAPS, 2% IPG buffer, 20 mM DTT). 3-10 NL IPG strips (24cm) were subjected to IEF electrophoresis. Focusing was carried out: (I) 30 V, 12 h, step; (II) 300V, 3h, step; (III) 300-600V, 1350 Vh, gradient; (IV) 600-1000V, 2400Vh, gradient; (V)1000-8000V, 13500 Vh, gradient; ( ) 8000 V, 56000 Vh. Prior to the second dimension, the IPG strips were equilibrated twice with solutions containing 100 mM Tris-HCl (pH 8.0), 6 M urea, 30% glycerol, 2% SDS, and a trace amount of bromophenol blue. DTT (1%) and IAM (4.5%) were added in the solutions of the first and second equilibration steps, respectively. IPG strips were placed on top of 12.5% SDS-PAGE gels precast with low-fluorescence glass plates. SDS-PAGE was carried out under the following conditions: 0.2 W/gel for 1 h; 0.4 W/ gel for 1 h; 1.8 W/gel for 15 h at 20°C.

Gel imaging and data analysis: Cy2, Cy3 and Cy5 labeled gels were individually imaged using excitation/ emission wavelengths of 488/520, 532/580 and 633/670 nm. Gel image was processed using DeCyder 6.5 (GE Healthcare, US). Spot detection was carried out using DIA module. BVA module was used for gel-to-gel matching, average abundance and statistics calculation. One Cy2-labeled internal standard spot map was served as the master gel image used to match different gel images (Alban *et al.*, 2003; Quin *et al.*, 2007; Richard *et al.*, 2006). The proteins spots of interest with an average ratio more than 1.5 or less than -1.5,$p<0.05$, were selected and picked up for protein identification by mass spectrometry.

Deep purple staining: The gel with a silanized spacer low-fluorescence glass plate was subjected to Deep Purple staining (GE Healthcare) that enhances identification accuracy by mass spectrometry (Liu *et al.*, 2008; Sun *et al.*, 2009). The gel was fixed with 1000 mL fixing solution (7.5% HAC, 10% methanol) overnight, washed with 750 mL washing solution (2.94gsodium bicarbonate, 31.8 g sodium carbonate, 750 mLH_2O), and stained with500 mL Deep Purple solutions for 1 h (Deep Purple:ddH_2O= 1:200) with vibration at RT in darkness. The gel was washed twice with500 mL of 7.5% HAC with vibration in darkness. Gel image was acquired using 488/610 nm.

Protein spots picking and in-gel digestion: Deep-Purple-stained gel image was matched to DIGE image, the spots of interest were robotically excised and digested according to our method (Liu *et al.*, 2008; Sun *et al.*, 2009). Briefly, the gel plugs were equilibrated with 25 mM ABC for 10 min and dehydrated with 10-min incubations with 100% ACN (twice). The dehydrated gel plugs were then incubated in 10 mM DTT at 56 °C for 45 min followed by induction 55 mM IAM for 45 min. Repeat twice the first wash and dehydrate steps. Protein was digested with porcine modified trypsin (Promega) in 25 mM ABC for 16 h at 37 °C. Tryptic peptides were extracted from gel in two cycles of 50% ACN, 1% FA.

Protein identification by mass spectrometry: An HPLC chromatography (Surveyor) and an LTQ mass spectrometer combined platform was used for HPLC-nESI-MS/MS. A nanoscale C18 analytical column (150 ×

0.075mm, Dionex)was set for HPLC. Mobile phase A was 5% ACN with 0.1% FA, mobile phase B was 95% ACN with 0.1% FA. Peptides were eluted at a flow rate of 260 nL/min with a linear gradient of 5–90% B over 50 min. Mass spectra were collected using data-dependent acquisition of one MS full scan (400 to 1700*m/z*) followed by MS/MS scans of the five most abundant ions. MS/MS spectra were interpreted using Turbo Sequest Bioworks. The peptide cross-correlation scores (Xcorr) of 1.9, 2.5, and 3.75 were set for charge states 1, 2, and 3. Protein probability was set $<10^{-3}$. Cut-off threshold of the number of matched peptides *per* protein was set two, additional peptides were included to maximize peptide coverage of identified protein (Liu *et al.*, 2008; Sun *et al.*, 2009).

MALDI MS protein identification was performed based on PMT (peptide mass fingerprinting) assay using a ProOTOF 2000 mass spectrometer according to our method (Liu *et al.*, 2006; Sun *et al.*, 2006). In-gel tryptic peptides of spots were desalted and concentrated through a ZipTip C18. Peptides eluted from tip were mixed with α-cyano-4-hydroxycinnamic acid (10 mg/ml) in 50% acetonitrile with 0.1% TFA at volume ratio of 1:1. Mass spectrometer was operated in a 16 kV positive mode with a*m/z* range of 700-4000.

SDS-PAGE and Western blotting: Harvested HaCaT and DNBS-treated HaCaT cells were washed with cold PBS 3 times, and were sonicated in ice-cold RIPA buffer (Santa Cruz, US) for 20 min. The supernatants were collected by centrifugation at 12,000 rpm for 15min at 4°C. The protein concentrations of samples were determined by Bradford Assay.

Same amount of proteins from each sample was fractionated by 12%SDS-PAGE and transferred onto nitrocellulose membranes.β-actin was used as the internal standard. Membranes were washed three times for 10 min with PBS-T (20 mM, pH 7.4, 100 mM NaCl, 0.5% Tween-20) and blocked with nonfat milk powder 5% milk PBS-T (0.5% Tween-20) for 1 h at RT. Being washed extensively with PBS-T, the membranes were then incubated with the horseradish peroxidase-coupled secondary antibodies and were developed by ECL according to the kit instructions (GE HealthCare, US) using a ChemiDoc™ MP image system (Bio-Rad, US). And the relative expression levels of identified proteins were quantified by the densitometry of visualized bands versus that of the internal standard using Image Lab software (Bio-Rad, US). The antibodies used were as follows: rabbit anti-human CALM3 polyclonal antibody (1:350, ProteinTech),rabbit anti-p23 monoclonal antibody (1:1200,Abcam), mouse anti-IL-18 monoclonal antibody (1:400, Abcam), rabbit anti-TCEB2 polyclonal antibody (1:2000, ProteinTech), goat anti-MYL6 polyclonal antibody (1:200, Santa Cruz), rabbit anti-BANF1 monoclonal antibody (1:2000, Abcam) and rabbit anti-RPL23 polyclonal antibody (1:600, Protein Tech).

RNA isolation and real-time PCR: We performed real-time PCR (qRT-PCR) to detect the mRNA expression levels of the corresponding genes of the 8 identified proteins most differentially expressed in HaCaT due to DNBS stimulations. In brief, total RNA was isolated from the cells using Trizol™ reagent (Life technologies, USA) according to the manufacturer's protocol. The reverse transcription was performed using the Prime Script™ RT reagent Kit with gDNA Eraser (TaKaRa, Japan), PCR was performed by Agilent M×3005P real-time PCR machine (Agilent, USA) with Fast Start universal SYBR Green Master (ROX) (Roche, Switzerland). PCR primers were designed using Oligo 7 software as listed in Table 3. ACTB was used as the internal standard. The mRNA levels of differentially expressed genes between HaCaT and DNBS-treated HaCaT cells were analyzed using the $2^{-\Delta\Delta CT}$ method.

RESULTS

2D DIGE gel patterns were consistent and reproducible. Over1200 protein spots were averagely resolved in each of the 3 gels, and over 800 protein spots were matched in all 3 gels. A comprehensive gel views of DIGE were shown in Fig.1, with gel images of Cy2-labelled internal standard (Fig. 1A), Cy3-labelleduntreated HaCaT (Fig. 1B), Cy5-labelledDNBS-treated HaCaT (Fig.1C) and overlaid gel image (Fig. 1D). Deep Purple-stained gel image was given in Fig. 1E. Deep Purple was used for gel post-staining as proteins were statistically more accurately identified by mass spectrometry with higher quality (Liu *et al.*, 2008; Sun *et al.*, 2009). DIA analysis of protein expression in DIGE gels produced 3-D representations of protein spots proportional in volume to the emission florescence intensity. Grounded on DeCyder analysis, the ratios of normalized spot intensities of DNBS treated HaCaTto untreated HaCaT cells were calculated. Nine spots showing more than 1.5- or less than -1.5-fold difference ($p<0.05$) were picked (numbered in DIGE image, Fig.1F).The volumes of 7 spots were increased and 2 spots were decreased for DNBS-treated HaCaT cells comparing to control cells (Table 2).

Eight unique proteins were identified by searching MS/MS data against *Homo sapiens* database derived from NCBInr database through TurboSequest Bioworks (Table 2).Among identified proteins, the 6 most up-regulated proteins were chromosome X open reading frame 26 (Cxorf26), calmodulin (CALM3), human co-chaperone P23 (PTGES3), smooth muscle and non-muscle myosin alkali light chain (MYL6) and breakpoint cluster region protein 1 (BANF1) and IL-18, the 2most down-regulated proteins were elongin B isoform alpha (TCEB2) and ribosomal protein

L23(RPL23).

Fig.2 shows a representative identification result for spot 5 of CALM3. Seven peptides, LTDEEVDEM*IR, VFDKDGNGYISAAELR, M*KDTDSEEEIREAFR, DT DSEEEIREAFR, MKDTDSEEEIR, LTDEEVDEMIR, E AFSLFDKDGDGTITTK and EADIDGDGQVNYEEFV QM*M*TAK were derived from MS data (*methionine oxidation, Fig. 2A). Fig. 2B is the representative MS/MS spectrum of VFDKDGNGYISAAELR. The peaks at mass-to-charge (m/z), 288.26, 417.16, 488.48, 599.39, 649.39, 759.49, 922.44, 979.50, 1094.52, 1151.48, 1266.51 and 1339.421 were the y series of fragment ions of y_2, y_3, y_4, y_5, y_6, y_7, y_8, y_9, y_{10}, y_{11}, y_{12} and y_{13}. The peaks at mass-to-charge (m/z), 605.32, 662.25, 777.30, 833.11, 997.37, 1110.37, 1468.49 and 1581.66 were the b series of fragment ions of b_5, b_6, b_7, b_8, b_9, b_{10}, b_{14} and b_{15}. The peaks 587.34 and 1249.71 were confirmed as dehydration fragment ions of b_5 and b_{12}, and 1076.62 and 1450.46 were confirmed as deamination fragment ions of y_{10} and b_{14} (Fig. 2B). Spots 3 and 4 were identified as PTGES3 (Table 2). Same protein was identified from different spots might be caused by protein isoforms and/or protein post-translational modifications.

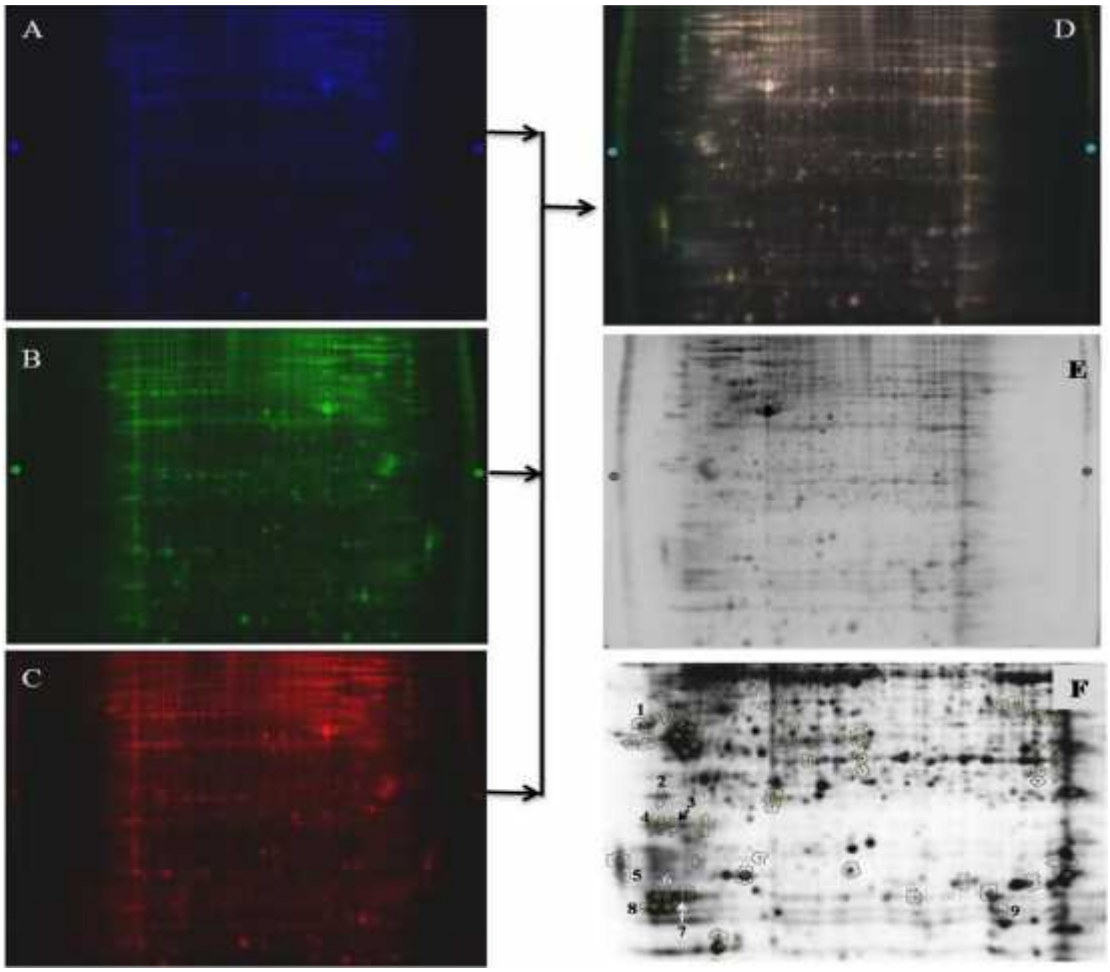

Figure 1. Representative images of 2D DIGE gels.

(A) gel image of Cy2-labelled internal standard; (B) gel image ofCy3-labelleduntreated HaCaT cell; (C) gel image of Cy5-labelled DNBS treated HaCaT cell; (D)overlaid gel image of Cy2-, Cy3- and Cy5-labelled protein extracts of HaCaT cells; E: gel image stained with Deep Purple; (F) differentially expressed protein spots.

The identified proteins were associated with HaCaT DNBS damage, which also implicates they might be potential targets for skin cell damage and skin diseases caused by chemical carcinogens. To validate the protein identification results by proteomic approach, the densitometric quantification results for expression levels detected by Western blotting (WB) for PTGES3, CALM3, TCEB2, IL18, BANF1, MYL6 and RPL23 are shown in Fig.3. WB assays indicated that the levels of PTGES3, CALM3, TCEB2, IL18, BANF1, MYL6 and RPL23 were about 2.0-, 1.8-, 0.59-, 1.6-, 2.7-, 2.1- and 0.53-folds in DNBS-stimulated HaCaT cells relative to HaCaT (Fig.

3). The WB validation results were consistent with proteomic results of the expression fold changes of 1.6 and 1.5 (up-regulation, spots 3 and 4) for PTGES3, 1.8 of CALM3 (up-regulation, spot 5), 2.0 of TCEB2 (down-regulation, spot 6), 1.5 of IL18 (up-regulation, spot 2), 1.8 of BANF1 (up-regulation, spot 8) 1.5 of MYL6 (up-regulation, spot 7) and 1.5 of RPL23 (down-regulation, spot 9), as shown in Table 2. The changes measured by WB demonstrate similar trends as reported by 2-DE DIGE. Meanwhile, the mRNA levels of 8 identified corresponding proteins show same expression trends as their protein levels. qRT-PCR results showed the mRNA expression levels of CXorf26, IL-18, PTGES3, CALM3, MYL6 and BANF1 increased to be ~2.8-, 3.3-, 4.6-, 3.9-, 2.2- and 5.8-fold in DNBS-treated HaCaT cells compared to control group HaCaT cells. While, the mRNA levels of TCEB2 and RPL23 in DNBS-treated HaCaT cells were only ~32% and 42% in HaCaT cells due to the stimulation of DNBS. qRT-PCR results are also consistent with DIGE and Western blotting results.

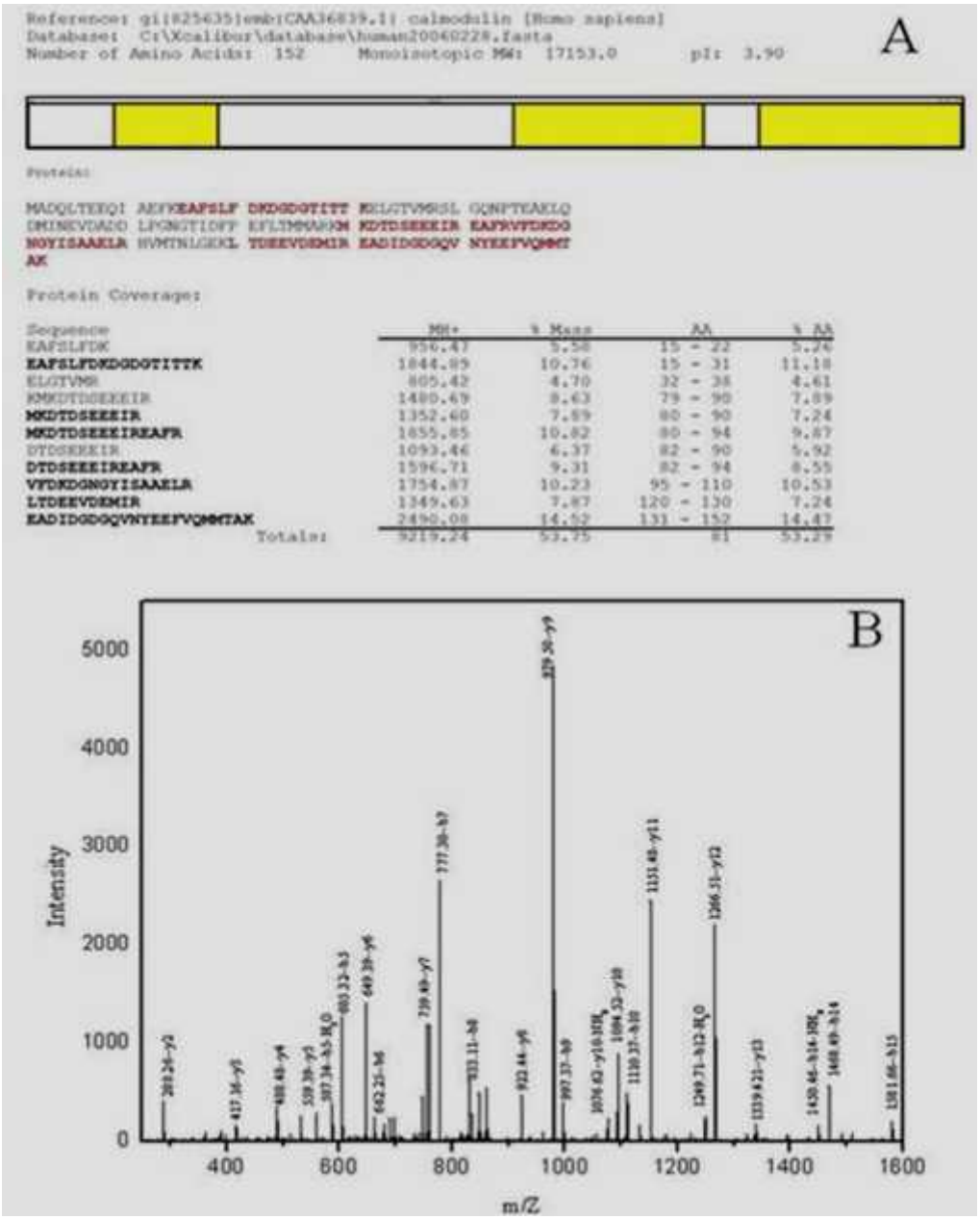

Figure 2. MS identification result for gel spot 1128.

(A) Overall identification result for 1128. (B) MS/MS spectrum of identified peptide VFDKDGNGYISAAELR.

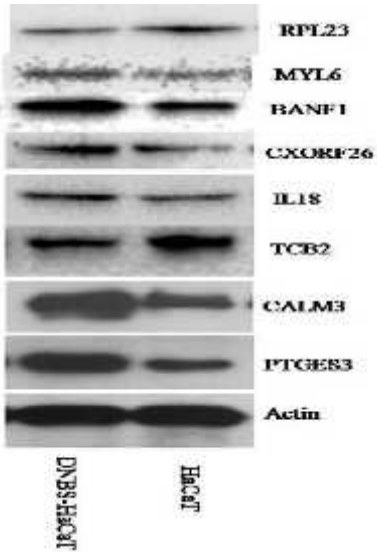

Figure 3. Western validations of identified proteins.

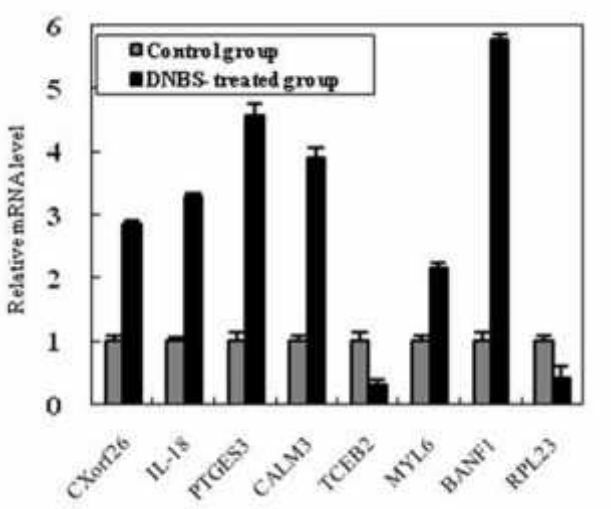

Figure 4. qRT-PCR assay of expression levels of corresponding genes for identified proteins.

Table 1.Compositions and gel assignments of the six samples for 2D DIGE.

Gel	Cy2 (Ins) [a]	Cy3 labeling	Cy5 labeling	Unlabeled protein[b]
1	50 μg	50 μg C1	50 μg DNBS1	150 μg
2	50 μg	50 μg DNBS2	50 μg C2	150 μg
3	50 μg	50 μg C3	50 μg DNBS3	150 μg

[a]8.33 (50/6, 6 means the 6 samples) μg of each samples from C1, C2, C3, DNBS1, DNBS2 andDNBS3 were pooled together; [b]25 μg of each samples from C1, C2, C3, DNBS1, DNBS2andDNBS3.

Table 2. Up- and down-regulated Proteins in DNBS-Treated group Compared with Control Group

Spot No.	Protein Description	Gene Symbol	Accession No.[a]	Peptides Matched	Sequence Coverage (%)	Deregulation (P<0.05)*
1	Chromosome X open reading frame 26	CXorf26	30354299	13/32	51	1.5 ↑
2	Interferon-gamma inducing factor precursor	IL18	1899242	13/47	52	1.5 ↑
3	Human co-Chaperone P23	PTGES3	9257073	4/62	38	1.6 ↑
4	Human Co-Chaperone P23	PTGES3	9257073	7/48	64	1.5↑
5	Calmodulin	CALM3	825635	8/27	54	1.8 ↑
6	Transcription elongation factor B polypeptide 2 isoform	TCEB2	6005890	5/14	35	-2.0 ↓
7	Myosin light polypeptide 6	MYL6	16924329	10/30	53	1.5 ↑
8	Breakpoint cluster region protein 1	BANF1	3002951	7/17	37	1.8 ↑
9	Ribosomal protein L23	RPL23	38571606	2/4	24	-1.5 ↓

* Protein fold changes between DNBS-treated HaCaT and control HaCaT cells. 1.5↑ and -1.5↓ represent 50% increase and 50% decrease in protein expressions for treated sample than the control; [Δ]represents the gene identification number. Note: Spots 3 and 4 were identified by MALDI MS; Spots 1,2,5,6,7,8 and 9 were identified by HPLC-EST-MS/MS.

Table 3. Designed primers of target genes

Gene	Primer
CXorf26	F:5′-GAACTCAAGTCAGAATCAGCC-3′ R:5′-AGAACAATCTAGTCGCAGCAA-3′
IL-18	F:5′-GACTGTAGAGATAATGCACCC-3′ R:5′-GAGATAGTTACAGCCATACCTC-3′
PTGES3	F:5′- AAACTTACATTCAGTTGTCTCGG -3′

CALM3	R:5′- GCCAGATTCTCCTTTTCGT-3′ F:5′- CATTGACTTCCCGGAGTTCCT-3′ R:5′- CATTGACTTCCCGGAGTTCCT-3′
TCEB2	F:5′- CAGTCAAACAGCACGGCCACA -3′ R:5′- ATTGGCACTGCTTCCCGAGT-3′
MYL6	F:5′- CAGAACCCTACCAACGCCGAG-3′ R:5′- TTCCTTGTCAAACACCCGAAG-3′
BANF1	F:5′- AACCTCCCAAAAGCACCGAGA -3′ R:5′- TCTTCATCTTTCTTTAGCACCAG-3′
RPL23	F:5′- CAGTCAAGAAAGGCAAACCAG -3′ R:5′- ATGGCAGAACCTTTCATCTCG -3′
ACTB	F:5′- CAGCCATGTACGTTGCTATCCAGG -3′ R:5′- AGGTCCAGACGCAGGATGGCATG -3′

DISCUSSION

DIGE technique is one of the most reliable quantification proteomic methods (Liu *et al.*, 2008; Sun *et al.*, 2009). Two different samples and a pooled standard are separated in a single DIGE gel that minimizes the reproducibility problem. The quantization of protein expression profile can be rapidly and accurately achieved based on the emission fluorescence intensities of Cy2, Cy3 and Cy5. The inclusion of pooled standard sample on each gel facilitates precise gel-to-gel matching, as same matched complete spot map is present on each gel (Liu *et al.*, 2008; Sun *et al.*, 2009).

Among 8 protein candidates, CALM3 was reported to be associated with skin burns and wound healing, keratinocytes proliferation and migration. Rare study has been addressed on the associations of remaining proteins with skin cell damages and skin diseases. CALM3 was involved in terminal keratinocyte differentiation (Rosenthal *et al.*, 2000). It inhibits the proliferation of dividing human keratinocytes. CALM3 mRNA level decreased by 30% and 50% in primary human endothelial cells treated with UV-irradiation for 1 h and 3 h (Watson *et al.*, 2000). It was down-regulated in HeLa cells in response to UVC-irradiation, while went back to normal after 24 h of UV-irradiation treatment. CALM3 level change correlated to DNA replication activity and synchronizes DNA synthesis (Rosenthal *et al.*, 2000; Watson *et al.*, 2000 Watson *et al.*, 2000). Interestingly, our results showed it was up-regulated in response to DNBS stimulation. Further study is required for its action mechanism.

The rest identified proteins were for the first time reported to be associated with skin cell damage. Myosin is a motor protein playing a key role in cell migration and posterior cell retraction. MYL was abnormally expressed in UVC-irradiated HeLa cells (Decker *et al.*, 2003). Myosin II phosphorylation was important for wounded keratinocytes cell migration and epidermis wound healing (Betapudi *et al.*, 2010; Iocono *et al.*, 2000). Myosin-10 could be activated by calmodulin-like protein to function in skin differentiation and wound re-epithelization of human keratinocytes (Bennett *et al.*, 2009). DNBS stimulation affected MYL6 expression in HaCaT cells. MYL6 inspot7 was up-regulated to 1.5-fold of that in control HaCaT cells (Table 2).

UV-induced immune suppression is a risk factor for skin cancer development (Hur *et al.*, 2010; Katiyar 2007; Yanti and Hwang, 2010). The normal level of cytokines interleukin 8 (IL-8) was critical for skin wound healing. IL-8 down-regulation in wounded skin or unhealed skin resulted in decreased keratinocyte replication. However, the elevated IL-8 levels contributed to retarded wound healing (Iocono *et al.*, 2000). IL-12 removes or repairs UV-induced DNA damage in skin (Katiyar 2007). IL-18 plays important roles in cancers, in autoimmune and infectious diseases (Gracie *et al.*, 2003). IL-18 was up-regulated in HaCaTcells following DNBS stimulation, suggesting its association with skin cell damage or even skin diseases.

Heat shock proteins (HSPs) are involved in protein misfolding prevention and repair, and cell injuries. HSP27, HSP70 and HSP90 were up-regulated in UVB-irradiated HeLa cells counteracting the damage through interactions with DNA repair enzymes (Mendez *et al*., 2000; Mori-Iwamoto *et al*., 2007; Yang *et al*., 2009).As an important modulator of HSP90 activity, PTGE3 is a prominent target in cell apoptosis inhibiting the aggregation of denatured proteins (Gausdal *et al.*,).Our proteomic data indicated PTGES3 was up-regulated to 1.6-fold, which was the direct response from HaCaT against DNBS. It might be a potential marker for skin cell damage by chemical carcinogens.

There are no study reported on the associations of TCEB2, CXorf26, BANF1 and RPL23, as identified differentially expressed in HaCaT against DNBS stimulation (Table 2), with skin cell damages or skin diseases. These protein candidates might be potential indicators for skin cell damage and new targets in chemical carcinogens-induced skin diseases.

Conclusions: Chemical carcinogens are playing important roles in the development of human skin

diseases. CXorf26, IL18, PTGES3, CALM3, TCEB2, MYL6, RPP2, BANF1 and RPL23were most differentially expressed in HaCaT proteome following DNBS stimulation. CALM3 was associated with skin burn wound healing, keratinocytes proliferation and migration. PTGES3 up-regulation in HaCaT cells might help cell to remove and repair misfolded proteins caused by DNBS stimulation. The abnormal expression of IL-18 implicates an immune response in HaCaT against possible inflammation induced by DNBS.

Most of these identified protein candidates in HaCaT cells were for the first time revealed responsible for DNBS stimulation damage. The precise roles of them in skin cell against chemical carcinogens need investigating. They are potential effective protection indicators for skin diseases induced by chemical carcinogens.

Acknowledgements: This work was supported by grants from National Natural Science Foundation of China (81171957, 81272186, 81100722), Outstanding Youth Scholar Growth Project in University and College of Liaoning (LJQ2011094), Liaoning BaiQianWan Talent Project (2012921015) and United Natural Science Fund of Liaoning Province (2014023047). We thank Dr. Mark Chance and Dr. Kevin Cooper from Case Western Reserve University, Cleveland, OH, USA, for experiment and technique support.

REFERENCES

Alban, A., S. O. David, L. Bjorkesten, C. Andersson, E. Sloge, and I. Currie (2003). A novel experimental design for comparative two-dimensional gel analysis: two-dimensional difference gel electrophoresis incorporating a pooled internal standard. Proteomics 3: 36–44.

Betapudi, V., V. Rai, and J. R. Beach (2010). Novel regulation and dynamics of myosin II activation during epidermal wound responses. Exp. Cell Res. 316: 981–991.

Bennett, R. D., A. S. Mauer, M. R. Pittelkow, and E. E. Strehler (2009). Novel regulation and dynamics of myosin II activation during epidermal wound responses. J. Invest. Dermatol. 29:765–769.

Cuzzocrea, S., M. C. Mcdonald, and E. Mazzon (2001). Calpain inhibitor I reduces colon injury caused by dinitrobenzene sulphonic acid in the rat. Gut 48:478–488.

Damian, D. L., C. R. Patterson, M. Stapelberg, J. Park, R. S. Barnetson, and G. M. Halliday (2008). UV radiation-induced immunosuppression is greater in men and prevented by topical nicotinamide. J. Invest. Dermatol. 128: 447–454.

Decker, E. D., Y. Zhang, R. R. Cocklin, F. A. Witzmann, and M. Wang (2003). Proteomic analysis of differential protein expression induced by ultraviolet light radiation in HeLa cells. Proteomics 3: 2019–2027.

Gausdal, G., B. T. Gjertsen, K. E. Fladmark, H. Demol, J. Vandekerckhove, S. O. Doskeland (2004). Caspase-dependent, geldanamycin-enhanced cleavage of co-chaperone p23 in leukemic apoptosis. Leukemia 2004; 18: 1989-96.

Gracie, J. A., S. E. Robertson, and I. B. Mcinnes (2003). Interleukin-18. J. Leukoc. Biol. 73: 213–224.

Harper, M (2004). Assessing workplace chemical exposures: the role of exposure monitoring. J. Environ. Monit. 6:404–412.

Hensbergen, P., A. Alewijnse, J. Kempenaar, R. C. van der Schors, C. A. Balog, A. Deelder, G. Beumer, M. Ponec, and C. P.Tensen (2005). Proteomic profiling identifies an UV-induced activation of cofilin and destrin in human epidermis. J. Invest. Dermatol. 124: 818–824.

Hopper, B. D., J. Przybyszewski, H. W. Chen, K. D. Hammer, and D. F. Birt (2009). Effect of ultraviolet B radiation on activator protein 1 constituent proteins and modulation by dietary energy restriction in SKH-1 mouse skin. Mol. Carcinog. 48: 843–852.

Housman, T. S., S. R. Feldman, P. M. Williford, A. B. Fleischer, N. D. Goldman, J. M. Acostamadiedo, and G. J. Chen (2003). Skin cancer is among the most costly of all cancers to treat for the Medicare population. J.Am. Acad. Dermatol. 48: 425–429.

Hur, S., Y. S. Lee, H. Yoo, J. H. Yang, and T. Y. Kim (2010). Homo isoflavanone inhibits UVB-induced skin inflammation through reduced cyclooxygenase-2 expression and NF-kappa B nuclear localization. J. Dermatol. Sci. 59:163–169.

Iocono, J. A., K. R. Colleran, and D. G. Remick (2000). Interleukin-8 levels and activity in delayed-healing human thermal wounds. Wound Repair Regen. 8: 216–225.

Katiyar S. K (2007). UV-induced immune suppression and photocarcinogenesis: chemoprevention by dietary botanical agents. Cancer Lett. 255: 1–11.

Liu, S., M-Z. Sun, and F. T. Greenaway (2006). A novel plasminogen activator from *Agkistrodon blomhoffii Ussurensis* venom (ABUSV-PA): purification and characterization. BBRC 348: 1279–1287.

Liu, S., M-Z. Sun, J. Tang, Z. Wang, C. Sun, and F. T. Greenaway. High-performance liquid chromatography/nano-electrospray ionization tandem mass spectrometry, two-dimensional difference in-gel electrophoresis and gene microarray identification of lymphatic

metastasis-associated biomarkers. Rapid Commun. Mass Spectrom. 22: 3172– 3178.

Mendez, F., M. Sandigursky, W. A. Franklin, M. K. Kenny, R. Kureekattil, and R. Bases (2000). Heat-shock proteins associated with base excision repair enzymes in HeLa cells. Radiat. Res. 153:186–195.

Mori-Iwamoto, S., Y. Kuramitsu, S. Ryozawa, K. Mikuria, M. Fujimoto, S. Maehara, Y. Maehara, K. Okita, K. Nakamura, and I. Sakaida (2007). Proteomics finding heat shock protein 27 as a biomarker for resistance of pancreatic cancer cells to gemcitabine. Int. J. Oncol. 31:1345–1350.

Petrova, A., L. M. Davids, F. Rautenbach, and J. L. Marnewick (2011). Photoprotection by honeybush extracts, hesperidin and mangiferin against UVB-induced skin damage in SKH-1 mice. J. Photochem. Photobiol. B. 103:126–139.

Quin, G. G., A. C. Len, F. A. Billson, and M. C. Gillies (2007). Proteome map of normal rat retina and comparison with the proteome of diabetic rat retina: new insight in the pathogenesis of diabetic retinopathy. Proteomics 7: 2636–2650.

Richard, E., L. Monteoliva, S. Juarez, B. Perez, L. R. Desviat, M. Ugarte, and J. P. Albar (2006). Quantitative analysis of mitochondrial protein expression in methylmalonic acidemia by two-dimensional difference gel electrophoresis. J. Proteome Res. 5:1602– 1610.

Rijnierse, A., A. S. Koster, and F. P. Nijkamp (2006). Critical role for mast cells in the pathogenesis of 2,4-dinitrobenzene-induced murine colonic hypersensitivity reaction. J. Immunol. 176: 4375 –4384.

Rosenthal, D. S., C. M. Simbulan-Rosenthal, S. Iyer, W. J. Smith, R. Ray, and M. E. Smulson (2000). Calmodulin, poly(ADP-ribose) polymerase and p53 are targets for modulating the effects of sulfur mustard. J. Appl. Toxicol. 20: S43–S49.

Sun, M-Z., S. Liu, and F. T. Greenaway (2006). Characterization of a fibrinolytic enzyme (Ussurenase) from *Agkistrodon blomhoffii Ussurensis* snake venom: Insights into the effects of Ca^{2+} on function and structure. BBA Protein and Proteomics 1764:1340–1348.

Sun, M-Z., S. Liu, J. Tang, Z. Wang, X. Gong, C. Sun, and F. T. Greenaway (2009). Proteomics analysis of two mice hepatocarcinoma ascites syngeneic cell lines with high and low lymph node metastasis rates provide potential protein markers for tumor malignancy attributes to lymphatic metastasis. Proteomics 9: 3285–3302.

Vicentini, F, T. R. Simi, J. O. Del Ciampo, N. O. Wolga, D. L. Pitol, M. M. Iyomasa, M. V. Bentley, and M.J. Fonseca (2008). Quercetin in w/o microemulsion: *in vitro* and *in vivo* skin penetration and efficacy against UVB-induced skin damages evaluated *in vivo*. Eur. J. Pharm. Biopharm. 69:948–957.

Watson, C. A., C. M. Chang-Liu, and G. E. Woloschak (2000). Modulation of calmodulin by UV and X-rays in primary human endothelial cell cultures. Int. J. Radiat. Biol. 76: 1455–1461.

Yang, J., X. Liu, P. Niu, Y. Zou, and Y. Duan (2009). Correlations and co-localizations of Hsp70 with XPA, XPG in human bronchial epithelia cells exposed to benzolpyrene. Toxicology 265:10–14.

Yanti, A and J. K. Hwang (2010) Effects of macelignan isolated from *Myristica fragrans*on UVB-induced matrix metalloproteinase-9 and cyclooxygenase-2 in HaCaT cells. J. Dermatol. Sci. 57:114–122.